Journal of Harbin Engineering University
ISSN: 1006-7043

Vol 46 No. 3
March 2025

Investigation of Emission Characteristics of Rice Husk Briquettes Fuel enriched with croton megalocarpus oil

Mamadou II Diallo, Robert Kiplimo, Josephat K. Tanui, Peter Obara Oketch
Department of Mechanical and Mechatronic Engineering, Pan-African University, Institute for Basic Sciences, Technology and Innovation, Nairobi, 6200-00200.
Department of Marine Engineering and Maritime Operation, Jomo Kenyatta University of Agriculture and Technology, P.O. Box 62000 – 00200, Nairobi, Kenya.
Department of Mechanical Engineering, Dedan Kimathi University of Technology, Private Bag 10143, Nyeri, Kenya.
Department of Mechanical Engineering, Jomo Kenyatta University of Agriculture and Technology, P.O. Box 62000 – 00200, Nairobi, Kenya.

Abstract

This study investigates the emission characteristics of rice husk briquettes enhanced with croton megalocarpus oil (CMO) to assess their potential as a sustainable biofuel. Seventeen experimental tests with different combinations of particle size, air-mass flux, and CMO absorption rates were set using Box Behnken Design (BBD) methodology. Three levels of each of these factors were considered in the design. These parameters were tested within a fixed bed combustion system to evaluate their impact on CO2, CO, NO_x, and SO_x emissions. The results indicate that emissions of CO, CO_2, NO_x, and SO_x vary significantly with changes in air mass flux, particle size, and absorption rate. CO emissions decrease with increasing air mass flux due to enhanced combustion efficiency, whereas they increase with smaller particle sizes, likely due to incomplete combustion. CO_2 emissions are primarily influenced by absorption rate, with higher absorption rates leading to lower emissions as fuel oxidation improves. NO_x emissions increase with rising air mass flux and smaller particle sizes due to higher combustion temperatures that promote nitrogen oxidation. SO_x emissions are significantly affected by both air mass flux and particle size, with larger particle sizes and higher fluxes promoting better sulfur oxidation and reducing emissions. The statistical analysis confirms that air mass flux has the most significant impact on CO and NO_x emissions, while absorption rate plays a dominant role in CO_2 emissions. Particle size is particularly influential in modifying SO_x emissions. These findings demonstrate that CMO-enriched briquettes could substantially mitigate the environmental impact of biomass fuels by enhancing combustion efficiency and reducing key pollutants. This underlines their viability as a cleaner alternative in energy production, advocating for further development and implementation.

Keywords: Absorption Rate, Croton megalocarpus oil, Rice Husk Briquettes, Emission Characteristics,

1. Introduction

The combustion of biomass resources, such as rice husk briquettes, has attracted significant attention due to their potential as a renewable and environmentally sustainable energy source. A thorough understanding of the emission profiles of various gas species is essential for assessing the environmental impact of biomass combustion and formulating strategies to minimize harmful emissions. Biomass combustion occurs in several distinct stages, including heating, devolatilization, homogeneous reactions, and char oxidation. During the heating phase, moisture in the fuel evaporates, and the surface temperature rises until ignition is achieved. The devolatilization stage involves the thermal breakdown of dried biomass, generating both volatile compounds and char. The volatile components, consisting of gases and tars, undergo exothermic homogeneous reactions, further increasing the bed temperature. Depending on the combustion conditions, nitrogen oxides (NO_x) and sulfur oxides (SO_x) may be released during this phase. Finally, in the char combustion phase, heat and gaseous emissions are produced. However, incomplete combustion, channelling, and short residence times can lead to undesirable emissions and inefficiencies in the process [1].

In Kenya, rice farming is primarily concentrated in Kirinyaga, Busia, and Kisumu counties, where the total yearly output is roughly 50,000 tons [2]. With the population's increasing dependence on rice as a staple and the government's proactive stance on boosting agricultural outputs through diverse programs, there lies a significant potential to enhance rice cultivation. This advancement in sustainable rice production could

be leveraged as a source of renewable energy, transforming the biomass into various forms such as solid pelletized fuels, liquid fuels, or syngas through thermal, chemical, or biological processes [2]. Pelletized rice husks present a viable option for biomass combustion, but a comprehensive examination of their emission profiles and the impact of critical factors such as particle size, air-mass flux, and absorption rate processes is essential. Typically, these husks are transformed into densified fuel through the application of high compressive forces using reciprocating pistons. This method can be expensive due to the substantial energy required to operate pressurizing equipment. In some instances, the husks are carbonized before densification, which reduces the need for high compressive forces. This is often facilitated by the addition of binders to enhance compaction [3]. Carbonization improves the calorific value of the fuel by releasing volatile compounds during pyro-gasification and increasing the carbon content of the fuel [4]. This method is particularly advantageous in Africa, where solar energy can sufficiently dry the pelletized fuels, providing a sustainable income-generating activity for youth and women groups.

Lubwama et al., [3], [5] evaluated the appropriateness of both raw and carbonized rice husk briquettes for household use. Their findings indicated that briquettes made from biochar exhibited higher calorific values and contained fewer volatiles. Notably, their research identified a gap in determining the emission levels to assess the suitability of these briquettes for residential use. Additionally, they noted that the combustibility and ignitability of the carbonized briquettes were diminished, attributing this to inadequate heat transfer within the briquettes.

The burning of biomaterials like rice husk briquettes releases a mix of pollutants including NO_x, SO_x, C_xH_y, and CO into the atmosphere. The levels of these emissions are influenced by the fuel's morphological characteristics, the operational conditions, and the design of the [5], [6], [7].

The emissions generated from biomass burning are critical in assessing its environmental impact. Carbon monoxide, a byproduct of incomplete combustion, poses substantial health risks. CO2 emissions exacerbate climate change by elevating greenhouse gas concentrations in the atmosphere. Significant emissions of NO_x are instrumental in the degradation of ground-level ozone and the formation of acid rain, while SOx emissions can lead to respiratory issues and environmental damage. Previous research has indicated that the process of carbonization affects these emissions; an increase in carbon content typically results in higher NO_x and SO_x levels due to elevated combustion temperatures, while simultaneously reducing the presence of unburned hydrocarbons [8]. The importance of substituting fossil fuels with biomass to mitigate greenhouse gas emissions, specifically carbon dioxide CO_2, has been highlighted [9]. It has been pointed out that CO_2 emissions from renewable biomass are almost offset by the CO_2 absorbed during the growth cycle of the biomass. Research also underscores the benefits of carbonization, a process that augments biomass by boosting its energy density and decreasing its moisture content, thereby reducing sulfur dioxide SO2 emissions during combustion when compared to unprocessed biomass [9].

Studies on co-firing, which involves the simultaneous burning of renewable fuels such as biomass with primary fuels like coal, natural gas, or furnace oil, are ongoing [10], [11]. These investigations primarily aim to reduce harmful emissions through the combined combustion of biomass and coal. Recent research in Europe and the United States has demonstrated that this practice not only benefits the environment but also enhances the economic efficiency of power generation. Co-firing tests typically show a decrease in SO_2 and NO_x emissions, dependent on the type of biomass used. Additionally, the overall CO_2 emissions are lower, as biomass is considered CO_2-neutral. Since most biomass fuels contain minimal or no sulfur, co-firing with coal can further reduce net SO2 emissions, a particularly valuable feature when used with high-sulfur coals. The alkaline ash produced during biomass combustion also helps capture some of the SO_2 emissions. Moreover, woody biomass generally contains significantly less nitrogen by mass compared to coal, which can be advantageous. Co-firing allows for the use of less expensive fuels, potentially lowering fuel costs depending on the processing expenses associated with the biomass. Furthermore, blending different types of

biomass with coal can also mitigate soil and water pollution [10] .

The incorporation of liquid fuels into briquette fuels offers comparable benefits. The absorption of croton megalocarpus oil into briquette fuel enhances the briquette's calorific value. This increase in calorific value leads to reduced daily fuel consumption while also improving the combustion characteristics of fixed bed reactor. Croton megalocarpus oil, a bio-based fuel, can be derived from the Croton megalocarpus tree and used directly. This integration into briquette fuel thus presents an effective way to utilize this renewable resource efficiently. In this research, briquettes enriched with Croton megalocarpus oil were utilized, representing a novel approach to briquette fuel use. These Croton megalocarpus oil-enhanced briquettes were combusted in a fixed bed reactor.

Exploring the emission characteristics of carbonized rice husk briquettes enriched with croton megalocarpus oil is vital for fostering sustainable biomass utilization, particularly in addressing pressing environmental concerns associated with biomass energy production. This research contributes to the development of cleaner energy solutions that mitigate climate change impacts while offering valuable insights for enhancing biomass combustion techniques. However, the emission dynamics of rice husk briquettes enriched with croton megalocarpus oil during fixed bed combustion are not thoroughly understood, importance a significant gap in current knowledge. This study addresses this gap by examining the effects of combustion of carbonized rice husk briquettes enriched with croton megalocarpus oil on emission patterns and related health risks, thereby informing strategies to reduce emissions and promote sustainable energy practices.

The objective of this study was to analyze the emissions of CO_2, CO, NO_x, and SO_x during the combustion of carbonized rice husk briquettes enriched with croton megalocarpus oil. Focusing on the quantification of CO, CO_2, NO_x, and SO_x emissions, this research is critical for identifying effective emission control strategies that can be applied in real-world scenarios. Understanding these emissions is essential for developing approaches that enhance air quality and public health outcomes.

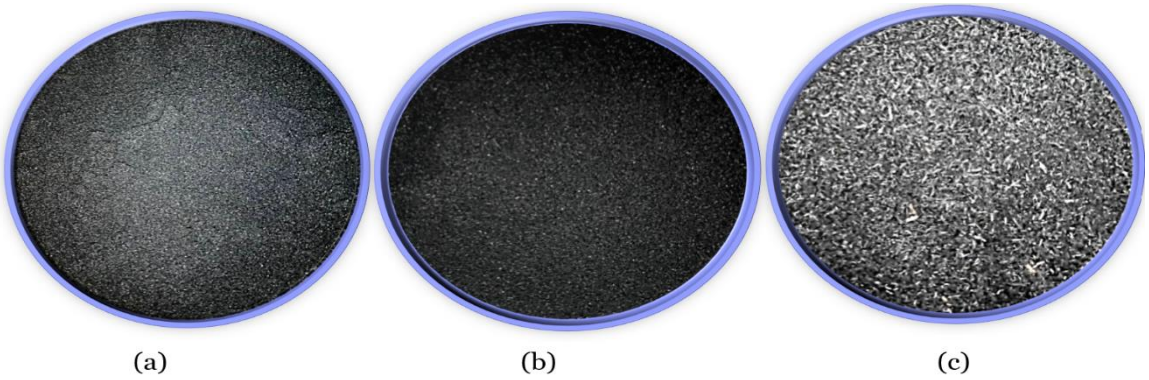

Figure 1: Carbonized rice husks; (a) 0.3 mm, (b) mm (c) 0.9 mm, (d) 1.5 mm.

2. Methodology

2.1. Briquette production process

The rice husks utilized in this research were obtained from local rice growers in Mwea, Kirinyaga, central Kenya. Locally sourced sugarcane molasses from Thika Town, Kiambu County, Kenya, was used as a binder to improve the structural stability of the briquettes. Dried raw rice husks were converted into biochar using a carbonizer made from a steel drum with a 200-liter capacity and a height-to-diameter ratio of 2:1. The drum featured air-regulating openings, each measuring 0.02 m across, to manage airflow during the carbonization process. The rice husks were ignited at the top of the drum, and the lid was closed to stop material loss. The air-control openings were blocked with mud to restrict oxygen access, promoting the pyro-gasification process inside the carbonizer [12]. According to Guo et al. [6], the ideal temperature range for producing biochar suitable for briquettes is between 400 and 500°C, with a biomass retention period of about 3 hours. In this research, the carbonization temperature was intentionally kept under 400°C. To address the reduced temperature and achieve full carbonization, the duration was increased to 4 hours, meeting the criteria for effective biochar production while accommodating the particular operational circumstances. The preparation of fuel

samples started with the threshing of the biomass, followed by sieving to separate particle size into distinct size categories. Particle size with mean particle sizes of 0.3 mm, 0.9 mm, and 1.5 mm were investigated. **Figure 1(a)- (c)** displays examples of fuels with these sizes.

In the Engineering Workshop at Jomo Kenyatta University of Agriculture and Technology, a screw extruder briquetting machine was utilized to create cylindrical briquettes measuring 38 mm in diameter, as shown in **Figure 2 (a).** The briquettes were subsequently sectioned into 40 mm lengths for every sample batch. **Figure 2 (b)** shows the briquettes created with a binder ratio of 6.6 wt% and particle sizes of 0.3 mm, 0.9 mm, and 1.5 mm. These values were chosen based on suggestions from earlier studies by Chirchir et al., [13] and Kipngetich et al., [12], which indicated that a binder ratio lower than 10 wt% offered adequate binding for briquettes while reducing non-combustible residues and not significantly raising ash content. To achieve a uniform and consistent blend of rice husk/molasses, 10% water by total weight was added during the preparation of the mixture. This method improved the integration of the binder and elevated the quality of the produced briquettes.

2.2. Preparation of briquette enriched with croton megalocarpus oil

The croton megalocarpus oil utilized in the experiments was obtained commercially from TRIPPLE E Engineer's Enterprise based in Nakuru, Kenya. Essential traits of the oil, such as density and viscosity, played a vital role in determining its absorption efficiency into the biomass. The properties of the croton megalocarpus oil used in this study are shown in **Table 1**.

Table 1. Properties of croton megalocarpus oil

Parameters	CMO
Viscosity at 40°C (mm^2/s)	23.187
Density at 23°C (g/cm^3)	0.896
Calorific value (MJ/kg)	41,180

The preparation of carbonized rice husk briquettes for the fixed-bed reactor experiments was carried out with meticulous precision to ensure consistency in fuel properties. Each briquette was individually weighed using a high-precision electronic balance with an accuracy of ±0.01 g to maintain uniform mass across all samples. To eliminate excess moisture while preserving the structural integrity of the briquettes, they were subjected to controlled drying in an oven at 105°C for one hour. This standardized drying process effectively reduced the initial moisture content to approximately 6.4%, ensuring optimal conditions for Croton megalocarpus oil (CMO) absorption. Following the drying process, the briquettes were immersed in CMO-filled 10-liter containers, each containing precisely 3.6 kg of briquettes. To guarantee accurate fuel-to-oil ratios, the briquettes and oil were carefully weighed using a precision electronic balance. The oil was gradually introduced into the containers, facilitating efficient absorption by the briquettes. Once the absorption process was complete, the briquettes were carefully strained to remove any excess oil, ensuring consistency in fuel composition.

Figure 2. Briquette production process: (a) Briquette making machine and (b) samples of briquettes produced at 6.6 wt% binder ratio.

They were then evenly spread on a flat surface and air-dried at room temperature for two days, allowing the absorbed oil to integrate uniformly into the biomass.

To determine the amount of CMO uptake, 60 g samples of carbonized rice husk briquettes were placed in individual containers, with CMO absorbed at controlled increments. These samples were subjected to different residence times to analyze the absorption dynamics. The weight of

each sample was recorded before and after oil absorption, enabling the calculation of the percentage weight increase due to biofuel uptake. Three levels of oil absorption rate were investigated; 12%, 18% and 24%. as illustrated in **Figure 3**. Specifically, briquettes enriched with CMO at 18% are shown in **Figure 4**.

2.3. Fuel Sample Properties

The properties of CMO-enhanced briquettes were evaluated through proximate and ultimate analyses to determine their composition and energy potential. Proximate analysis, conducted at the JKUAT laboratory, examined key parameters such as moisture content, volatile matter, fixed carbon, and ash content, providing crucial insights into the fuel characteristics of CMO-enriched briquettes. The moisture content was measured using an oven-drying method in

accordance with ISO 18134-2:2017-03E, while volatile matter was determined following ISO 18123:2016-01. The ash content was analyzed based on ISO 18122:2015, and fixed carbon was calculated using the ASTM D-3172-73 method.

For ultimate analysis, which quantifies elemental

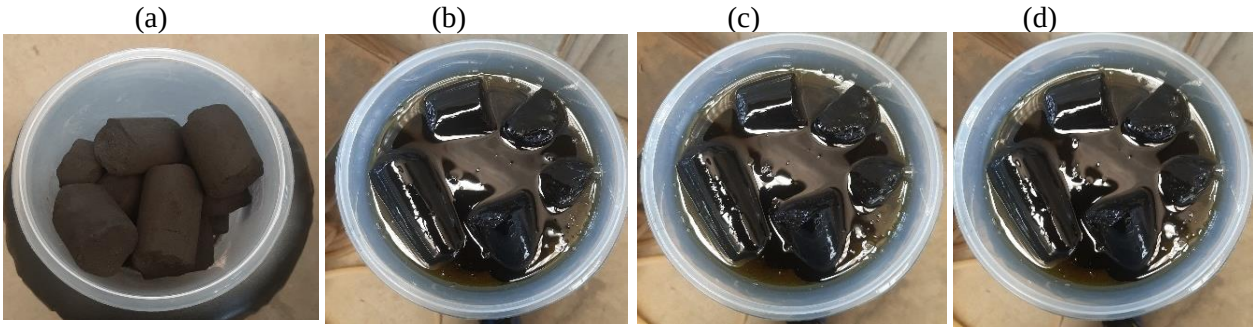

Figure 3. Briquette absorption with CMO at Different concentrations (Particle Size: 0.9 mm)

Raw briquettes (a)., (b) 12%., (c) 18%., (d) 24%

Figure 4. Briquettes enriched with CMO at 18%

composition, testing was performed at the East African Laboratory in Upper Hill, Kenya using a FlashSmart™ Elemental Analyzer (CHNS-O model) with a precision of 0.3 mg. This analysis measured carbon, hydrogen, nitrogen, and sulfur content in accordance with ISO 16994:2016, while oxygen content was determined by difference. Additionally, the gross calorific value (GCV) of the briquettes was assessed at the JKUAT laboratory using a C200-type oxygen bomb calorimeter with a precision of 0.2%, following the ISO 17225-6 standard. These analyses provided a comprehensive understanding of the combustion performance and energy potential of the CMO-enhanced briquettes, ensuring their suitability as a sustainable biofuel option.

2.4. Experiment setup

All experiments were conducted using a fixed-bed experimental setup, as depicted in **Figure 5**. This system comprises five main components: the fixed-bed reactor, temperature data acquisition system, emission sampling unit, fuel mass weighing scale, and airflow measurement device. The combustion chamber is a vertically positioned cylindrical structure, with a height of 540 mm and an internal diameter of 160 mm. Designed for thermal efficiency and durability, the chamber consists of four protective layers: an inner furnace wall, a 40 mm refractory cement layer with a thermal conductivity of 0.86 W/m·K [14], a 2 mm mild steel sheet, and an 18 mm aluminum silicate cotton fiber insulation layer. As noted by Lienhard and John [14], aluminum silicate cotton fiber has a thermal conductivity of approximately 0.055 W/m·K at 400 K, making it an effective insulator. The convective heat transfer coefficient (h) for air is between 10–20 W/m²·K under natural convection conditions [15]. Based on these thermal parameters, an outer radius of 276 mm was determined to provide adequate insulation for the reactor [16].

The system's air intake was designed to ensure uniform distribution through a perforated base plate, made from 1Cr18Ni9Ti stainless steel, a material capable of withstanding temperatures up to 1400°C [16]. The plate features 66 strategically placed openings, each 10 mm in diameter, to facilitate efficient airflow. Additionally, a circular plenum, tightly sealed to prevent air leaks and turbulence, was incorporated to enhance steady combustion performance.

To monitor mass loss during combustion, the fuel chamber's weight was continuously measured using a WT1503L electronic scale. The weight data was transmitted to a computer via an RS232 cable and systematically recorded in an Excel database for further analysis. Flexible tubing connections were employed to minimize external disturbances on the scale, ensuring accurate mass tracking throughout the experiment.

Temperature monitoring within the combustion chamber was achieved using seven Type-K thermocouples (TCs), capable of measuring temperatures between 0 and 1360°C. These thermocouples were installed at 50 mm intervals, as

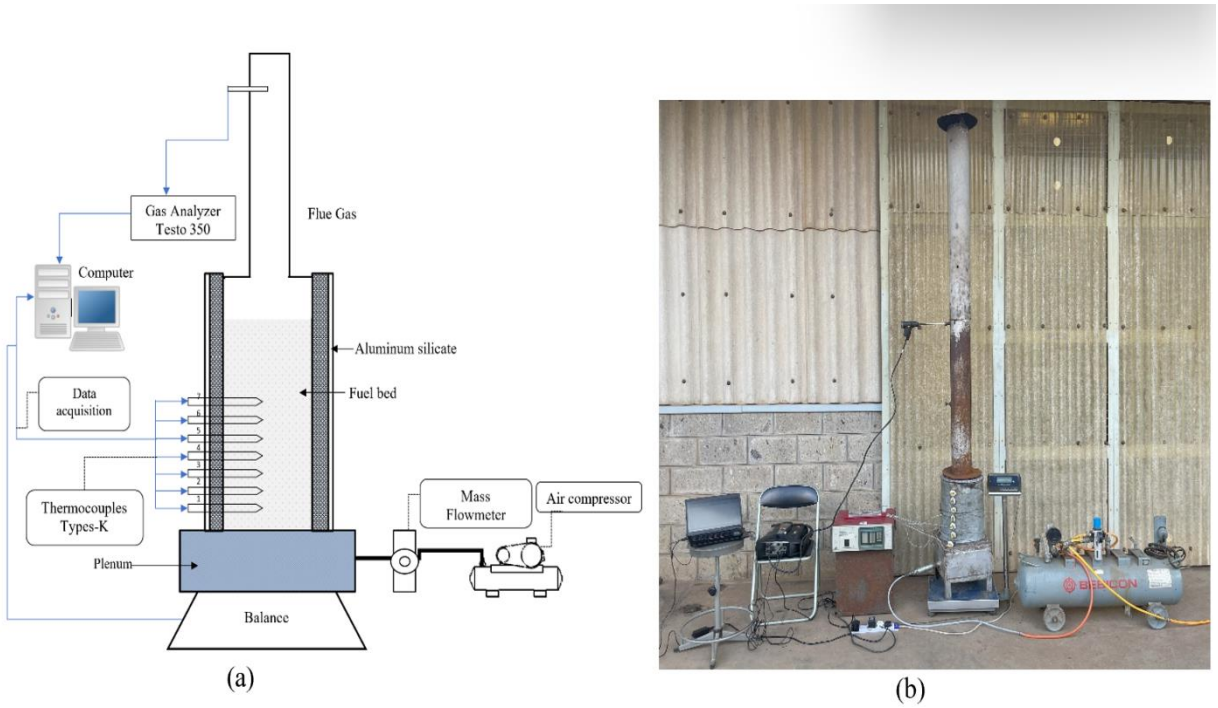

Figure 5: Experiment setup: (a) Schematic diagram, (b) Laboratory setup

summarized in **Table 2**, to track temperature gradients and reaction front propagation during drying, devolatilization, and char oxidation phases. Temperature data was collected using a BTM-4208SD data logger, which recorded measurements every 15 seconds, featuring a precision of ±0.4°C and a resolution of 0.1°C.

To regulate airflow, an LZB–25 float flow meter was utilized, offering a measurement range of 1–25 m^3/h with an accuracy of ±0.2 m^3/h. This precise control of air supply ensured optimal combustion conditions throughout the study.

For experimental consistency, the binder mass content was maintained at 6.6 wt%, while particle sizes were varied between 0.3 mm, 0.9 mm, and 1.5 mm to evaluate their influence on combustion dynamics. Additionally, oil absorption levels were set at 12%, 18%, and 24%, and air-mass fluxes were adjusted to 0.02 $kg/m^2 \cdot s$, 0.152 $kg/m^2 \cdot s$, and 0.284 $kg/m^2 \cdot s$. By incorporating different particle sizes, oil absorption rates, and air-mass flux variations, this study provided valuable insights into the synergistic effects of these parameters on the efficiency and performance of Croton megalocarpus oil-enriched briquettes.

Table 2. Thermocoupe locations

Thermocouple number	1	2	3	4	5	6	7
Distance from the grate (mm)	50	100	150	200	250	300	350

2.5. Emission Measurement

Emission measurements were conducted using the Testo 350 emission analyzer, a high-precision device equipped with a probe system for gas sampling. The analyzer maintains an accuracy within ±5%, ensuring reliable and consistent data collection. To obtain representative samples, a probe was carefully inserted into the emission source, allowing direct gas extraction. Before each measurement, the gas sampling system was thoroughly inspected and calibrated to prevent blockages and ensure optimal performance. During the sampling process, the probe was positioned near the exhaust pipe, where gases flowed through the probe and into the sampling system. Once collected, the gas samples were analyzed using advanced sensors and detectors integrated into the Testo 350, providing real-time assessments of multiple emissions. The system measured key gas components, including nitrogen oxides (NO_x), carbon monoxide (CO), carbon dioxide (CO_2), sulfur oxides (SO_x), and particulate matter, among others.

The measurement accuracy for each gas component was as follows:

- Carbon monoxide (CO): ±5% of the reading or ±10 ppm (whichever is greater) for concentrations between 0–2000 ppm; ±10% of the reading for 2001–40,000 ppm.
- Nitrogen oxides (NO_x): ±5% of the reading or ±5 ppm (whichever is greater) for concentrations between 0–500 ppm.
- Sulfur oxides (SO_x): ±5% of the reading or ±10 ppm (whichever is greater) for concentrations between 0–2000 ppm.
- Carbon dioxide (CO_2): ±0.3% accuracy.

2.6. Design of experiments

This study employed the Box–Behnken Design (BBD) approach to assess how combustion parameters influence the release of CO, CO_2, NOx, and SOx. As a variant of Response Surface Methodology (RSM), the BBD technique significantly reduced the cost and number of experimental runs required while effectively identifying optimal values for combustion properties [17], [18]. In a three-level factorial BBD, the total number of experiments was calculated using the **eq. (1).**

$$N = 2 * K(K-1) + CP \quad (1)$$

where K represents the number of factors, CP is the number of central points, and N is the total number of experiments. By leveraging this structured methodology, the study efficiently explored the influence of multiple variables. In this research, a total of 17 experiments were conducted. This included 12 experimental runs, with each factor evaluated at three distinct levels, and an additional five central point experiments for improved accuracy and reliability. All variables were changed at three distinct levels with equal increments of (-1, 0, +1) as stipulated by BBD. Absorption rate (%), air mass flux ($kg/m^2.s$), and particle size (mm) were labeled X_1, X_0, and X_2 respectively, with three corresponding values for these factors. Experimental points were created using the BBD

methodology with the Design-Expert 13 software program as illustrated in **Table 3**.

3. Results and discussions

3.1. Proximate and ultimate analysis

The data presented in **Table 4** underscores the significant impact of particle size on the properties of CMO-enriched briquettes. Smaller particle sizes (0.3 mm) demonstrate improved thermal properties, exhibiting lower moisture content (5.4%) and ash content (46.02%), alongside higher volatile matter (20.18%). Additionally, these finer particles achieve a notably higher heating value (HHV) of 35.4 MJ/kg, indicating greater energy density. Conversely, briquettes with larger particle sizes (1.5 mm) have a negative impact on thermal properties, characterized by higher ash content (47.6%), lower volatile matter (17.3%), and a reduced HHV of 32.5 MJ/kg. These findings suggest that larger particles hinder fuel utilization and heat transfer efficiency, leading to less effective energy conversion. Furthermore, carbon and hydrogen content, which are key contributors to energy release during combustion, also show a slight decrease with increasing particle size, further limiting the overall energy output.

Despite these variations, nitrogen and sulfur levels remain consistent across all particle sizes, indicating that NO_x and SO_x emissions are not significantly affected by particle size variations. This suggests that selecting smaller particle sizes in CMO-enriched briquettes can optimize combustion efficiency, increase energy output, and enhance overall fuel properties, making them a more efficient and sustainable biofuel choice.

Table 3. Actual and encoded values for input factors

Input Factors	**Codes of input factors**		
	X_1 (-1)	X_0 (0)	X_2 (+1)
Particle size (mm) (A)	0.3	0.9	1.5
Air mass flux ($Kg/m^2.s$) (B)	0.02	0.152	0.284
Absorption rate (%) (C)	12	18	24

Table 4. Proximate and ultimate analysis of the briquette enriched with CMO

Briquettes enriched with CMO			
Analysis	**Particle size (0.3 mm)**	**Particle size (0.9 mm)**	**Particle size (1.5 mm)**
Proximate (%)			
Moisture	5.4	5.5	5.6
Ash	46.0	47.4	47.6
Volatile Matter	20.2	18.0	17.3
Fixed Carbon	28.4	29.1	29.5
HHV (MJ/kg)	35.4	33.6	32.5
Ultimate (%)			
C	47.3	46.1	45.8
H	5.4	5.3	5.2
N	0.4	0.4	0.4
S	0.3	0.2	0.3
O	46.6	48.0	48.3

3.2. Emission characteristics

Table 5. Emissions characteristics as a function of input factors.

Factors				Responses			
Run	**Mass flux ($kg/m^2.s$)**	**Particle size (mm)**	**Absorption Rate (%)**	**Max carbon monoxide (CO)**	**Max nitrogen oxides (NO_x)**	**Max carbon dioxide (CO_2)**	**Max Sulfur oxides (SO_x)**
1	0.152	0.3	24	4031	48	1206	35
2	0.152	0.3	12	4762	58.2	1561	59.5
3	0.02	0.9	24	4681	66.3	347	38
4	0.152	0.9	18	2882	119	974	7.6
5	0.02	1.5	18	4145	39.9	1000	12.5
6	0.284	0.3	18	3172	137.3	1409	9.5
7	0.152	1.5	12	2305	47.1	1521	5
8	0.02	0.3	18	4708	171.8	623	65
9	0.152	0.9	18	2702	116	906	6.3
10	0.284	0.9	12	1972	164.8	1594	9
11	0.152	0.9	18	2902	109	792	15.3
12	0.284	0.9	24	1651	159	2131	6
13	0.152	0.9	18	2892	116	968	8.7
14	0.152	1.5	24	3332	37.2	304	12.5
15	0.02	0.9	12	4085	106.3	3379	51.5
16	0.152	0.9	18	2762	121	962	8.4
17	0.284	1.5	18	1271	233.6	213	5

Table 6. The emissions outcomes of ANOVA for all responses

Response: Maximum carbon monoxide (CO)						Response: Maximum nitrogen oxides (NO_x)				
Source	**Sum of Squares**	**df**	**Mean Square**	**F-value**	**p-value**	**Sum of Squares**	**df**	**Mean Square**	**F-value**	**p-value**
Model	1.83E+07	9	2.03E+06	89.09	< 0.0001	47922.8	9	5324.76	190.61	< 0.0001
A	3.95E+06	1	3.95E+06	173.06	< 0.0001	410.74	1	410.74	14.7	0.0064
B	1.14E+07	1	1.14E+07	500.28	< 0.0001	12051.19	1	12051.19	431.39	< 0.0001
C	40853.32	1	40853.32	1.79	0.2226	540.92	1	540.92	19.36	0.0032
AB	4.47E+05	1	4.47E+05	19.61	0.003	13019.17	1	13019.17	466.04	< 0.0001
AC	7.73E+05	1	7.73E+05	33.9	0.0006	0.0203	1	0.0203	0.0007	0.9792
BC	2.10E+05	1	2.10E+05	9.21	0.019	292.98	1	292.98	10.49	0.0143
A^2	1.07E+06	1	1.07E+06	46.73	0.0002	2326.37	1	2326.37	83.28	< 0.0001
B^2	209.54	1	209.54	0.0092	0.9263	11808.36	1	11808.36	422.69	< 0.0001
C^2	3.21E+05	1	3.21E+05	14.08	0.0071	8549.95	1	8549.95	306.06	< 0.0001
Residual	1.60E+05	7	22808.48			195.55	7	27.94		
Lack of Fit	1.27E+05	3	42317.07	5.18	0.0731	112.51	3	37.5	1.81	0.2856
Pure Error	32708.17	4	8177.04			83.04	4	20.76		
Cor Total	1.85E+07	16				48118.35	16			

Response: Maximum carbon dioxide (CO_2)						Response: Maximum sulfur oxides SO_x				
Source	**Sum of Squares**	**df**	**Mean Square**	**F-value**	**p-value**	**Sum of Squares**	**df**	**Mean Square**	**F-value**	**p-value**
Model	9194000	9	1022000	54.18	< 0.0001	6613.54	9	734.84	44.49	< 0.0001
A	387400	1	387400	20.55	0.0027	2244.5	1	2244.5	135.9	< 0.0001
B	1.44	1	1.44	0.0001	0.9933	2363.28	1	2363.28	143.09	< 0.0001
C	2069000	1	2069000	109.73	< 0.0001	140.28	1	140.28	8.49	0.0225
AB	619100	1	619100	32.83	0.0007	576	1	576	34.87	0.0006
AC	186000	1	186000	9.86	0.0164	256	1	256	15.5	0.0056
BC	3184000	1	3184000	168.88	< 0.0001	27.56	1	27.56	1.67	0.2374
A^2	715000	1	715000	37.92	0.0005	256.66	1	256.66	15.54	0.0056
B^2	385600	1	385600	20.45	0.0027	148.19	1	148.19	8.97	0.0201
C^2	1722000	1	1722000	91.34	< 0.0001	503.24	1	503.24	30.47	0.0009
Residual	132000	7	18855.93			115.61	7	16.52		
Lack of Fit	108500	3	36167.45	6.16	0.0557	66.56	3	22.19	1.81	0.2851
Pure Error	23489.19	4	5872.3			49.05	4	12.26		
Cor Total	9326000	16				6729.16	16			

Tables 5 and **Tables 6** present essential findings regarding the emission characteristics of carbonized rice husk briquettes enriched with croton megalocarpus oil (CMO). These tables provide a valuable understanding of the influence of key combustion parameters on pollutant emissions. **Table 5** systematically illustrates how variations in air mass flux, particle size, and absorption rate impact emissions of carbon monoxide (CO), carbon dioxide (CO_2), nitrogen oxides (NO_x), and sulfur oxides (SO_x). It serves as a comparative dataset, helping to identify optimal conditions for reducing harmful emissions. **Table 6** presents the results of the ANOVA (Analysis of Variance), evaluating the statistical significance of each parameter and their interactions. This analysis determines which factors have the most substantial effect on emission characteristics, aiding in the optimization of biomass combustion processes for cleaner energy production.

The statistical model for carbon monoxide (CO) emissions is highly significant, as indicated by an F-value of 89.09 and a p-value of < 0.0001, showing a strong correlation between the experimental factors and CO levels. Among these factors, air mass flux (B) shows the most significant impact on CO emissions, with an F-value of 500.28, highlighting its critical influence. Particle size (A) also shows a considerable effect, evidenced by an F-value of 173.06 as shown in the statistical analysis in **Table 6**. The interactions between these factors, particularly AB (mass flux and particle size) and AC (Particle size and absorption rate), are statistically significant, demonstrating synergistic effects on CO emissions. The quadratic terms for factors (A^2) and (C^2) are significant, emphasizing the nonlinear responses of CO emissions within the tested range. The residuals of the model are minor, and the lack of fit is not significant (p = 0.0731), suggesting that the model adequately captures the dynamics of the experiment as reflected in the provided statistical outputs **Eq. (2)**.

The analysis of nitrogen oxide (NO_x) emissions using ANOVA results presented in **Table 6** shows a significant model fit with an F-value of 190.61 and a p-value less than 0.0001, emphasizing the robust relationship between the examined factors and NO_x emissions. The most influential factor, air mass flux B, demonstrates a paramount effect with an F-value of 431.39, highlighting its critical role in controlling NO_x levels. Absorption rate (C) also shows a significant impact, with an F-value of 19.36. The interaction between these two factors, AB (mass flux and particle size), is notably impactful with an F-value of 466.04, indicating a strong synergistic influence on NO_x emissions. Additionally, the quadratic terms for both (B^2) and (C^2) reveal significant non-linear effects with F-values of 422.69 and 306.06, respectively. The model's residuals are minimal, and the lack of fit is not significant (p = 0.2856), confirming that the model adequately captures the dynamics of NO_x emissions within the

$$CO = 2827.98 - 702.418A - 1194.29B + 71.4609C - 334.422AB + 439.664AC - 229.148BC + 503.149A^2 - 7.0545B^2 + 276.219C^2 \quad (2)$$

scope of the studied variables as indicated by model **Eq.(3)**

$$NO_x = 116.197 - 7.16533\,A + 38.8124B - 8.2228C + 57.0508AB + 0.0712891AC + 8.5583BC - 23.5056\,A^2 + 52.9574B^2 - 45.0623C^2 \quad (3)$$

The ANOVA results for carbon dioxide (CO_2) emissions demonstrate a significant model with an overall F-value of 54.18 and a p-value less than 0.0001 as illustrated in the statistical analysis in **Table 6**, indicating a strong statistical correlation between the tested factors and CO_2 emissions. Absorption rate (C) stands out as the most influential, with an F-value of 109.73, highlighting its critical role in CO2 output. The relationship between air mass flux (B) and absorption rate (C) also significantly affects CO_2 levels, evidenced by an F-value of 168.88, suggesting a substantial synergistic effect. Additionally, the quadratic term for Factor (C^2) is notably impactful with an F-value of 91.34, illustrating the non-linear dynamics of its effect on CO_2 emissions. Particle size and its quadratic term (A^2) are also significant, with F-values of 20.55 and 37.92 respectively, indicating their importance in the emission process. The interactions AB and AC show significant effects as well, with F-values of 32.83 and 9.86 respectively. In contrast, air mass flux (B) alone demonstrates an almost negligible direct effect on CO_2 emissions, with an F-value of 0.0001. The residuals of the model are small, and the lack of fit, while not significant, shows a p-value of 0.0557, pointing to a generally good fit with potential for slight model improvement. This analysis underscores a complex interplay of factors affecting CO_2 emissions, with particular emphasis on the roles of absorption rate (C) and its interactions as indicated by model **Eq.(4)**.

$$CO_2 = 920.54 - 220.068A - 0.42375B - 508.562C - 393.402AB - 215.625AC + 892.25BC - 412.077A^2 + 302.635B^2 + 639.575C^2 \quad (4)$$

The ANOVA results for sulfur oxide (SO_x) emissions demonstrate a highly significant model, indicated by an overall F-value of 44.49 and a p-value of < 0.0001 as illustrated in the statistical analysis in **Table 6**. The data shows that particle size (A) and mass flux (B) are the most impactful, with F-values of 135.9 and 143.09 respectively, highlighting their dominant roles in influencing SO_x levels. Absorption rate (C), though less influential, still significantly affects SO_x emissions with an F-value of 8.49 and a p-value of 0.0225. The interactions between particle size and mass flux (AB) and particle size and absorption rate (AC) are also significant, with F-values of 34.87 and 15.5, respectively, indicating their substantial effects. Additionally, the quadratic terms for Factors (A^2) and (C^2) show significant non-linear impacts with F-values of 15.54 and 30.47 respectively. However, the interaction between mass flux and absorption rate (BC) is not significant, with an F-value of 1.67 and a p-value of 0.2374. The model's residuals are minimal, and the lack of fit is not significant (p = 0.2851), confirming that the model adequately captures the dynamics of SO_x emissions, effectively explaining the relationships and interactions among the factors studied as indicated by model **Eq.(5)**.

$$SO_x = 9.26 - 16.75\,A - 17.1875B - 4.1875C + 12AB + 8AC + 2.625BC + 7.8075A^2 + 5.9325B^2 + 10.9325C^2 \quad (5)$$

Figure 6(a)-(d) provides emission properties of carbonized rice husk briquettes enriched with CMO under varying mass flux and particle size conditions, keeping the absorption rate constant at 18%. **Figure 6(a)** shows that CO emissions are exceptionally high, particularly for smaller particle sizes of 0.3 mm emitting up to 4708 ppm and larger particle sizes of 1.5 mm emitting 4145 ppm, indicating inefficient combustion likely due to insufficient fuel burn and lower operational temperatures. In contrast, at a mass flux of 0.152

kg/m².s with a uniform particle size of 0.9 mm, emissions are somewhat moderated, ranging between 2702 and 2902 ppm, suggesting a more stable and efficient combustion process. However, at a higher mass flux of 0.284 kg/m².s, there is a significant decrease in emissions for particle size of 1.5 mm down to 1271 ppm, which points to improved combustion

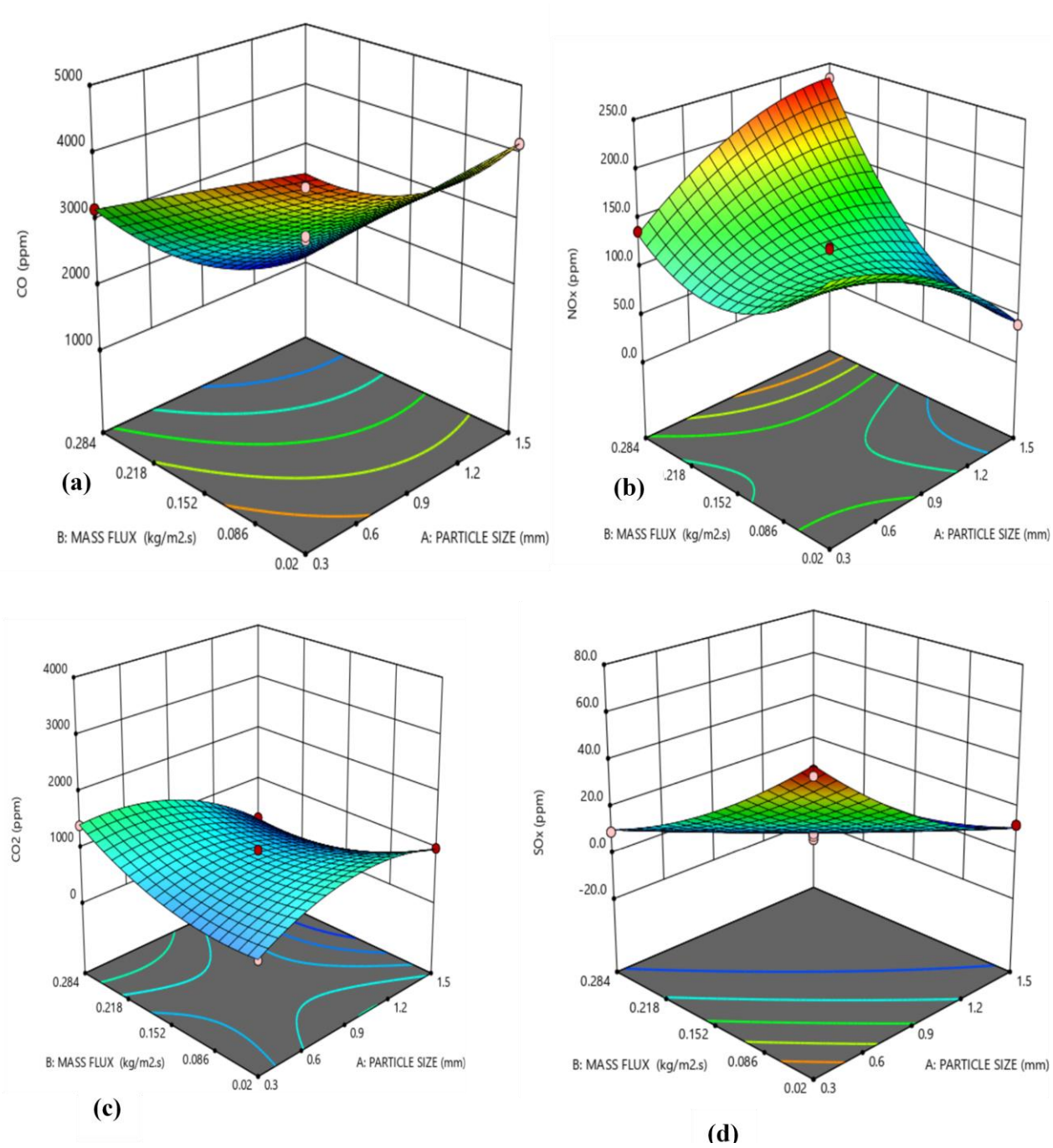

Figure 6 (a)-(d): Emission characteristics of carbonized rice husks briquettes enriched with CMO under a constant absorption rate of 18% by varying mass flux from 0.02-0.284 kg/m^2s and particle size from 0.3-1.5 mm.

efficiency through better heat retention and oxygen utilization. These results demonstrate that smaller particles tend to emit more CO at lower mass fluxes due to less efficient combustion, while larger particles achieve better combustion efficiency at higher fluxes.

Figure 6(b) reveals that NO_x emissions are significantly affected by particle size, with a particle size of 0.3 mm emitting substantially more NO_x, especially at a lower mass flux of 0.02 kg/m_2.s, due to increased surface area facilitating more intense nitrogen-oxygen reactions. In contrast, a larger particle size of 1.5 mm shows reduced NO_x levels under similar conditions, suggesting less effective combustion dynamics. As mass flux increases, NO_x emissions also rise peaking for larger particles at a higher mass flux of 0.284 kg/m².s, indicating that intensified combustion conditions enhance NO_x formation.

Figure 6(c) reveals that at a low mass flux of 0.02 kg/m².s, CO_2 emissions are higher for larger particle size of 1.5 mm at 1000 ppm, compared to 623 ppm for smaller particle size of 0.3 mm. This suggests that the larger particles achieve more complete combustion due to slower burn rates and better heat retention, allowing for more thorough carbon oxidation. For mass flux of 0.152 kg/m^2.s with a consistent particle size of 0.9 mm, CO_2 emissions are relatively stable, ranging from 792 to 974 ppm, indicative of an optimal combustion balance where the fuel is sufficiently oxidized without excessive or insufficient oxygen. Conversely, at a high mass flux of 0.284 kg/m^2.s, smaller particle size produce significantly higher CO_2 emissions of 1409 ppm, as the increased mass flux enhances oxygen availability, matching the fast reaction rates and promoting more complete combustion. However, for a larger particle size of 1.5 mm at this high mass flux, CO_2 emissions drop drastically to 213 ppm, likely due to slower heat transfer, resulting in incomplete combustion and reduced CO_2 output.

Figure 6(d) reveals that at a low mass flux of 0.02 kg/m².s, smaller particles of 0.3 mm emit significantly higher levels of SO_2 at 65 ppm, likely due to their increased surface area facilitating rapid oxidation of sulfur compounds in the fuel at lower combustion temperatures, leading to higher emissions. In contrast, larger particles of 1.5 mm at the same mass flux level produce lower emissions of 12.5 ppm, suggesting slower sulfur oxidation rates. At a mass flux of 0.152 kg/m².s with a uniform particle size of 0.9 mm, emissions stabilize between 6.3 and 15.3 ppm, Furthermore, at a high mass flux of 0.284 kg/m².s, emissions decrease even further, particularly for larger particles of 1.5 mm, where enhanced airflow and higher temperatures promote more efficient combustion processes and minimize SO_2 release.

Figure 7(a)-(d) explores the emissions properties of carbonized rice husk briquettes enriched with CMO across various particle sizes and absorption rates, maintaining mass flux at 0.152 kg/m^2s. **Figure 7(a)** reveals that smaller particles, particularly at a 0.3 mm size, exhibit increased CO emissions as absorption rates decrease, suggesting that rapid burn-off and insufficient time for complete combustion at lower absorption rates contribute to higher emissions. For particle sizes of 0.9 mm, CO emissions are relatively stable, indicating an optimal combustion environment where the fuel absorption and particle size effectively match the oxygen availability. However, larger particles of 1.5 mm show that higher absorption rates significantly increase emissions, highlighting a complex interaction where larger particle sizes may facilitate more complete combustion but also generate more emissions if not optimally managed. **Figure 7(b)** shows that small particles, when subjected to a decrease in absorption rate from 24% to 12%, exhibit an increase in NO_x emissions from 48 ppm to 58.2 ppm, suggesting that faster combustion and higher local temperatures, which are conducive to NO_x formation, are more prevalent at lower absorption rates. Particle sizes of 0.9 mm consistently produce higher emissions, ranging from 109 to 121 ppm at an 18% absorption rate, indicating that their optimal balance between surface area and volume sustains higher temperatures for longer durations, ideal for NO_x generation. Conversely, large particles show a marked decrease in emissions, down to 37.2 ppm at a 24% rate, as their slower burn rates and potentially lower peak temperatures are less favorable for NO_x production. **Figure 7(c)** reveals that small particles show an increase in CO_2 emissions from 1206 ppm to 1561 ppm as absorption rates decrease from 24% to 12%, suggesting rapid fuel consumption doesn't allow for complete carbon oxidation. In contrast, medium-sized particles maintain a more stable emission range between 792 ppm and 974 ppm at an 18% absorption rate, indicating optimal combustion conditions that balance rapid reaction and sufficient oxidation. Large particles exhibit a significant reduction in emissions, dropping to 304 ppm at a 24% absorption rate from 1521 ppm at 12%, due to slower combustion that enhances fuel and air integration for more complete carbon oxidation. **Figure 7(d)** reveals that smaller particles increase SO_x emissions from 35 ppm to 59.5 ppm as absorption rates decrease from 24% to 12%, suggesting that rapid surface reactions in

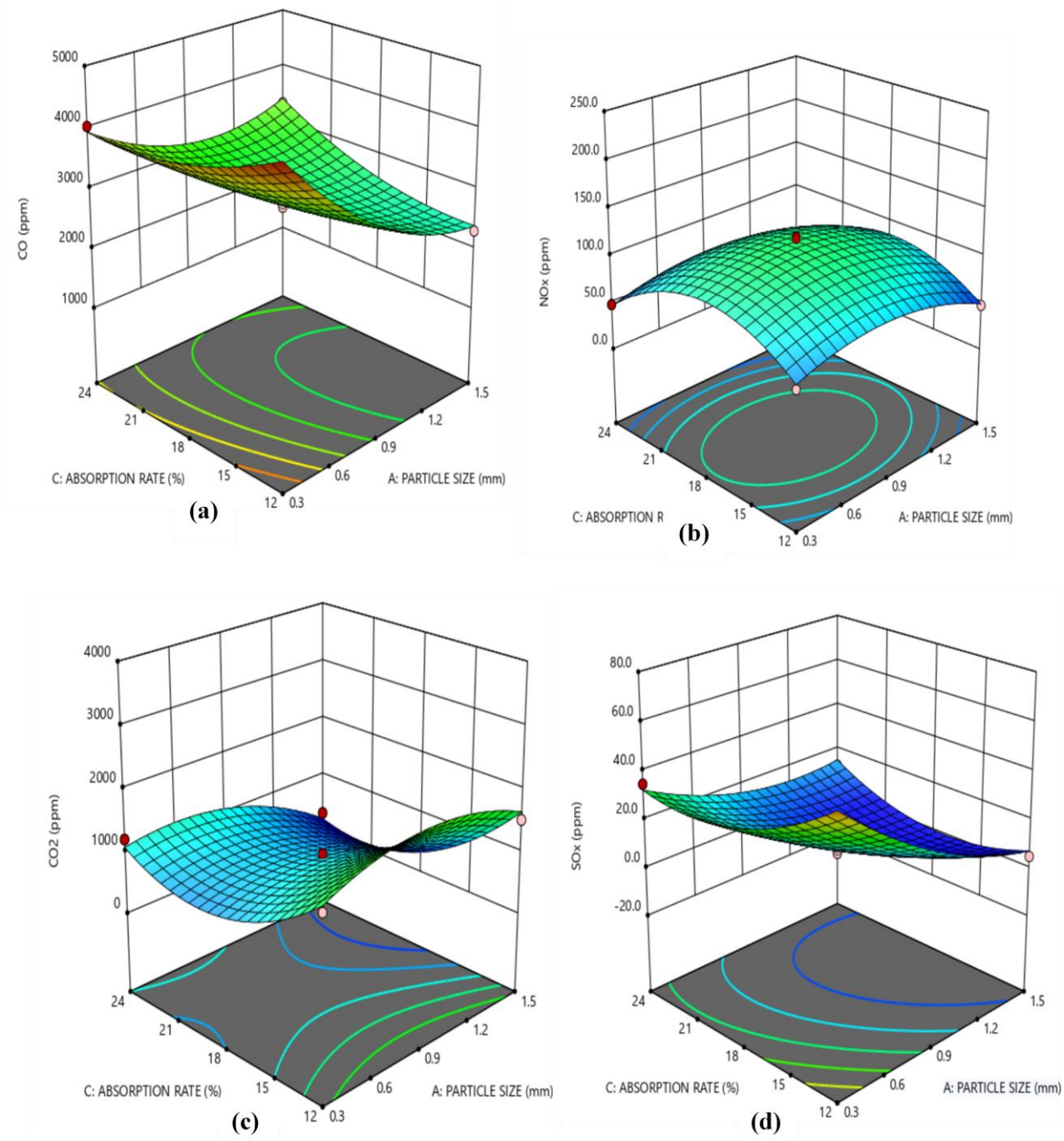

Figure 7 (a)-(d): Emission characteristics of carbonized rice husks briquettes enriched with CMO under a constant mass flux of 0.152 kg/m^2s by varying particle size from 0.3-1.5 mm and absorption rate of 12-24%.

smaller particles prevent the complete processing of absorbed sulfur, leading to higher emissions. Conversely, medium-sized particles show relatively

stable and low SO_x emissions between 6.3 ppm and 15.3 ppm at an 18% absorption rate, indicating balance for sulfur integration and conversion during combustion. Large particles, on the other hand, demonstrate a decrease in SO_x emissions to 5 ppm at a lower absorption rate of 12% and a slight increase to 12.5 ppm at a higher rate of 24%, likely due to slower combustion kinetics that allow more time for sulfur to be fully converted into less harmful compounds.

Figure 8(a)-(d) provides the emissions characteristics of carbonized rice husk briquettes enriched with CMO across different mass flux levels and absorption rates, keeping the particle size consistent at 0.9 mm. **Figure 8(a)** reveals that at the lowest mass flux of 0.02 kg/m².s, CO emissions are highest, recording 4681 ppm at a 24%

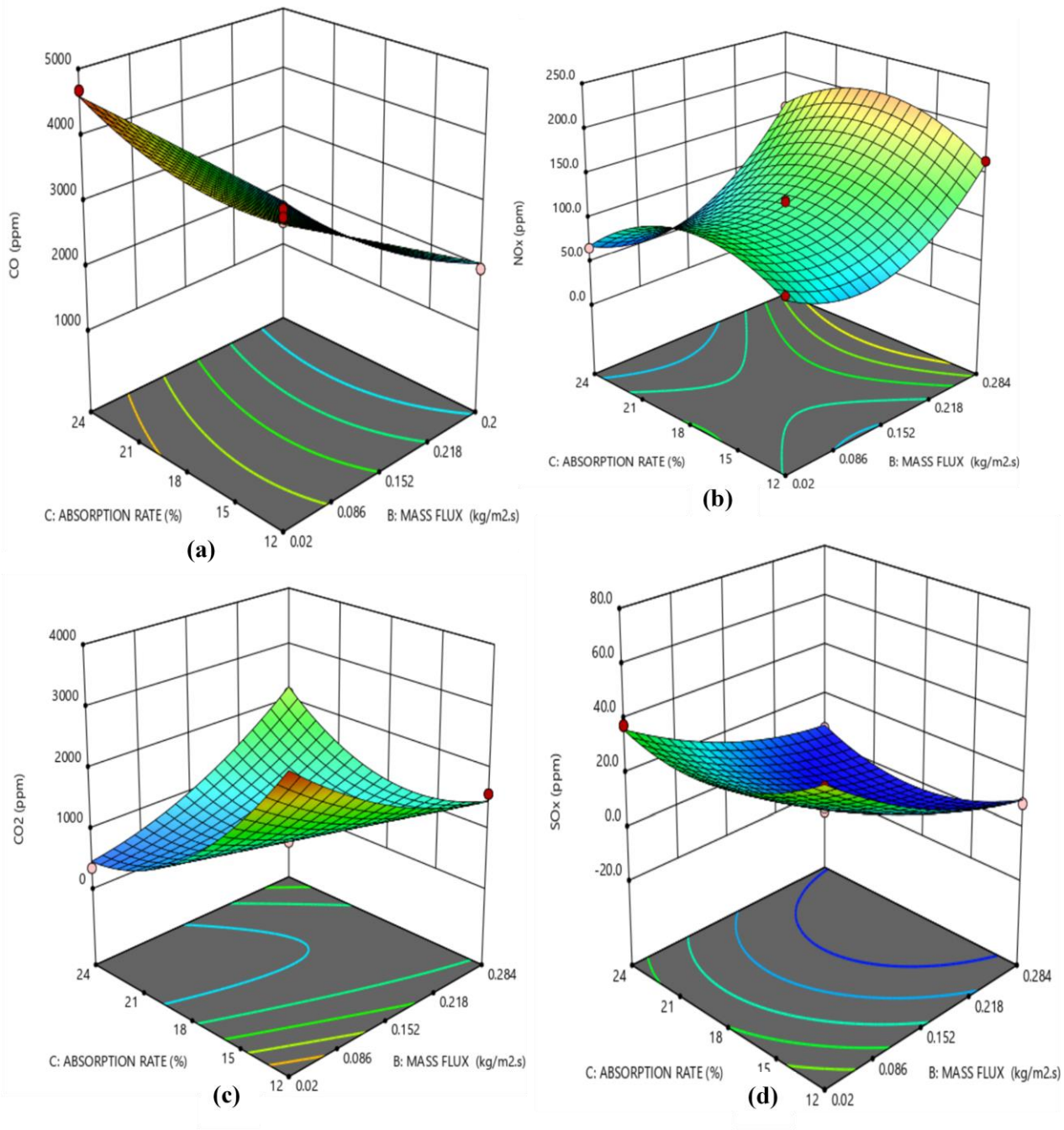

Figure 8 (a)-(d): Emission characteristics of carbonized rice husks briquettes enriched with CMO under a constant particle size 0.9 mm by varying mass flux from 0.02-0.284 kg/m^2s and absorption rate of 12-24%.

absorption rate and 4085 ppm at 12%, indicating insufficient oxygen for complete combustion. As the mass flux increases to 0.152

kg/m².s, emissions decrease significantly to a range of 2702 to 2902 ppm at an 18% absorption rate, suggesting a balance of fuel and oxygen that enhances combustion efficiency. At the highest mass flux of 0.284 kg/m².s, CO emissions drop further to 1972 ppm at a 12% absorption rate and 1651 ppm at 24%, underscoring that increased oxygen availability at higher flux levels promotes more complete combustion, resulting in lower emissions. **Figure 8(b)** exposes that at a low mass flux of 0.02 kg/m².s, NO_x emissions increase from 66.3 ppm to 106.3 ppm as the absorption rate decreases from 24% to 12%, suggesting that lower absorption rates may reduce combustion efficiency and increase NOx production. Mass flux of 0.152 kg/m².s, NO_x emissions are consistently higher,

ranging from 109 to 121 ppm at an 18% absorption rate, indicating that increased mass flux enhances combustion temperatures and oxygen mixing, which in turn promotes NO_x formation. Further increasing the mass flux to 0.284 kg/m².s leads to even higher emissions, peaking at 164.8 ppm at a 12% absorption rate, highlighting that higher mass flux conditions intensify the factors conducive to NO_x production despite the absorption rate. **Figure 8(c)** illustrates that at the lowest mass flux of 0.02 kg/m².s, CO_2 emissions exhibit considerable variation with absorption rates, peaking at 3379 ppm at a 12% rate and dramatically reducing to 347 ppm at a 24% rate. This indicates that higher absorption rates significantly improve carbon oxidation efficiency, particularly at lower flux levels. As the mass flux increases to 0.152 kg/m².s with an 18% absorption rate, emissions stabilize between 792 ppm and 974 ppm, suggesting a more balanced and efficient combustion process. However, at the highest mass flux of 0.284 kg/m².s, CO_2 emissions fluctuate once more, reaching 2131 ppm at a 24% rate and 1594 ppm at 12%. This variability underscores that while increased oxygen availability at higher fluxes generally enhances combustion completeness, it also leads to higher CO_2 emissions. **Figure 8(d)** illustrates how SO_x emissions respond to varying conditions of mass flux and absorption rates. At the lowest mass flux of 0.02 kg/m².s, SO_x emissions rise from 38 ppm at a 24% absorption rate to 51.5 ppm at a 12% rate, suggesting that lower absorption rates at minimal flux levels lead to increased emissions, likely due to inadequate processing of sulfur compounds. Conversely, at a medium mass flux of 0.152 kg/m².s with an 18% absorption rate, emissions are significantly lower and more consistent, ranging from 6.3 to 15.3 ppm. This stability indicates a more effective combustion environment for sulfur processing. At the highest mass flux of 0.284 kg/m².s, emissions decrease even further to 6 ppm at a 24% rate, as opposed to 9 ppm at a 12% rate, underscoring that higher mass flux and increased absorption rates substantially improve the conversion and oxidation of sulfur compounds, thus effectively reducing SO_x emissions.

4. Conclusion

The research demonstrated that particle size, air mass flux, and absorption rate significantly influenced CO, CO_2, NO_x, and SO_x emissions during the combustion of croton megalocarpus oil (CMO)-enriched rice husk briquettes. CO emissions decreased with higher air mass flux and absorption rates but increased with smaller particle sizes due to incomplete combustion. CO_2 emissions were primarily influenced by absorption rate, with higher absorption reducing emissions by optimizing fuel oxidation. NO_x emissions increased with air mass flux and smaller particle sizes at lower absorption rates due to higher combustion temperatures. SO_x emissions were significantly affected by particle size and air mass flux, with larger particles and higher flux promoting better sulfur oxidation and lower emissions, while lower absorption rates led to increased SO_x emissions. Among these factors, air mass flux had the most significant impact on CO, NO_x, and SOx emissions, while absorption rate was the dominant factor for CO_2. The interaction between particle size and air mass flux was also crucial in modifying emissions, whereas air mass flux had a negligible direct effect on CO^2 emissions, and the interaction between mass flux and absorption rate had minimal impact on SO_x.

Credit Contribution Statement for Authorship

M. Il Diallo: Conceptualization, Methodology, Research, Writing – Original draft. **R. Kiplimo**: Conceptualization, Methodology, Supervision. **J.K. Tanui**: Conceptualization, Methodology, Supervision. **P.O. Oketch**: Conceptualization, Methodology, Investigation, Supervision, Writing – Review & Editing.

Statement of Conflicting Interests

The authors state that there are no financial or personal conflicts of interest that may have affected the work outlined in this paper.

Acknowledgment

This study received financial backing from the Pan African University Institute for Basic Sciences, Technology, and Innovation.

References

[1] A. Williams, J. M. Jones, L. Ma, and M. Pourkashanian, “Pollutants from the combustion of solid biomass fuels,” Apr. 2012. doi: 10.1016/j.pecs.2011.10.001.

[2] P. Njogu, Y. Nemoto, and R. Kinyua, “Fabrication, optimization and purification of syngas from rice husks; A value chain addition strategy for rice farmers in Mwea, Kenya,” in *Proceedings of the Sustainable Research and Innovation Conference*, 2022, pp. 68–71.

[3] M. Lubwama, V. A. Yiga, and H. N. Lubwama, "Effects and interactions of the agricultural waste residues and binder type on physical properties and calorific values of carbonized briquettes," *Biomass Convers Biorefin*, vol. 12, no. 11, pp. 4979–4999, Nov. 2022, doi: 10.1007/s13399-020-01001-8.

[4] J. K. Tanui, P. N. Kioni, P. N. Kariuki, and J. M. Ngugi, "Influence of processing conditions on the quality of briquettes produced by recycling charcoal dust," *International Journal of Energy and Environmental Engineering*, vol. 9, no. 3, pp. 341–350, Sep. 2018, doi: 10.1007/s40095-018-0275-7.

[5] M. Lubwama and V. A. Yiga, "Characteristics of briquettes developed from rice and coffee husks for domestic cooking applications in Uganda," *Renew Energy*, vol. 118, pp. 43–55, Apr. 2018, doi: 10.1016/j.renene.2017.11.003.

[6] Z. Guo *et al.*, "Characteristics of biomass charcoal briquettes and pollutant emission reduction for sulfur and nitrogen during combustion," *Fuel*, vol. 272, Jul. 2020, doi: 10.1016/j.fuel.2020.117632.

[7] R. Yang, C. Ma, G. Chen, Z. Cheng, B. Yan, and M. Mansour, "Study on NOx emission during corn straw/sewage sludge co-combustion: Experiments and modelling," *Fuel*, vol. 285, Feb. 2021, doi: 10.1016/j.fuel.2020.119208.

[8] P. Kipngetich, J. K. Tanui, and R. Kiplimo, "The effect of carbonization on emissions of carbon, nitrogen and sulfur oxides from fixed bed combustion of rice husk briquettes," *Biomass Convers Biorefin*, 2023, doi: 10.1007/s13399-023-04685-w.

[9] R. G. Landers, K. Barton, S. Devasia, T. Kurfess, P. Pagilla, and M. Tomizuka, "A review of manufacturing process control," *J Manuf Sci Eng*, vol. 142, no. 11, p. 110814, 2020.

[10] A. Nuamah, A. Malmgren, G. Riley, and E. Lester, "5.05 - Biomass Co-Firing," in *Comprehensive Renewable Energy*, Elsevier, 2012, pp. 55–73. doi: 10.1016/B978-0-08-087872-0.00506-0.

[11] M. Kopczyński, J. A. Lasek, A. Iluk, and J. Zuwała, "The co-combustion of hard coal with raw and torrefied biomasses (willow (Salix viminalis), olive oil residue and waste wood from furniture manufacturing)," *Energy*, vol. 140, pp. 1316–1325, Dec. 2017, doi: 10.1016/j.energy.2017.04.036.

[12] M. Lubwama and V. A. Yiga, "Characteristics of briquettes developed from rice and coffee husks for domestic cooking applications in Uganda," *Renew Energy*, vol. 118, pp. 43–55, Apr. 2018, doi: 10.1016/j.renene.2017.11.003.

[13] D. K. Chirchir, D. M. Nyaanga, and J. M. Githeko, "effect of binder types and amount on physical and combustion characteristics," 2013. [Online]. Available: http://www.ijerst.com/currentissue.php

[14] I. V. Lienhard and H. John, *A heat transfer textbook, Phlogiston press,*. 2005.

[15] F. P. Incropera, D. P. DeWitt, T. L. Bergman, and A. S. Lavine, *Fundamentals of heat and mass transfer*, vol. 6. Wiley New York, 1996.

[16] P. Kipngetich, R. Kiplimo, J. K. Tanui, and P. C. Chisale, "Optimization of combustion parameters of carbonized rice husk briquettes in a fixed bed using RSM technique," *Renew Energy*, vol. 198, pp. 61–74, Oct. 2022, doi: 10.1016/j.renene.2022.07.130.

[17] M. A. Bezerra, R. E. Santelli, E. P. Oliveira, L. S. Villar, and L. A. Escaleira, "Response surface methodology (RSM) as a tool for optimization in analytical chemistry," Sep. 15, 2008, *Elsevier*. doi: 10.1016/j.talanta.2008.05.019.

[18] B. Lela, M. Barišić, and S. Nižetić, "Cardboard/sawdust briquettes as biomass fuel: Physical-mechanical and thermal characteristics," *Waste Management*, vol. 47, pp. 236–245, 2016, doi: 10.1016/j.wasman.2015.10.035.